Composition-induced phase-transition splitting in cuprous selenide

Z. Vučić, O. Milat, V. Horvatić, and Z. Ogorelec
Institute of Physics of the University, Zagreb, Yugoslavia
(Received 28 May 1980; revised manuscript received 24 June 1981)

The nature of the phase transition to the superionic phase of cuprous selenide has been investigated by measuring thermal expansion, electron diffraction, and electronic conductivity. The degenerate nature of the transition has been demonstrated by introducing controlled deviations from stoichiometry. The origin of this first-order phase transition is interpreted in terms of the formation of a modulated ion distribution along the [111] cubic axis.

The purpose of the present investigation has been to determine the effect of compositional changes on the nature of the phase transitions from the low-temperature–low-conducting phase to the high-temperature–superionic (SI) phase of cuprous selenide. Here we present experimental evidence for composition induced phase transition splitting in the narrow composition range between Cu_2Se and $Cu_{1.955}Se$.

We have found[1] that the room-temperature (β) phase of stoichiometric cuprous selenide (Cu_2Se) is a superstructure of the rhombohedrally deformed fcc substructure of the high-temperature (α) phase. The superstructure itself can be described as an ordered cation subsystem within the "zinc-blende framework" of immobile Cu and Se ions—the cage. At T_c a discontinuous transition from β to α phase was observed. This transition corresponds to an order-disorder transition of the cation subsystem and a rhombohedral to cubic symmetry transformation of the cage.

For nonstoichiometric samples ($Cu_{2-x}Se$) two close transitions were detected.[2] Above the lower (continuous) one, the cation subsystem can be considered to be disordered as shown by ionic conductivity data.[3] The higher transition still retained discontinuous character but surprisingly without any detectable change in ionic conductivity.[3]

It is our intention to analyze structural and physical aspects of phase transitions of $Cu_{2-x}Se$ in order to understand the stoichiometric case. We believe that this is of general interest since there are several other SI conductors[4] which have complicated discontinuous phase transitions, but these have not yet been prepared with variable stoichiometry.

The present investigations were carried out with a most careful composition control and uniform thermal treatment of samples. The sample preparation has been described earlier.[2]

We have measured the temperature dependence of the linear thermal expansion coefficient as a function of composition on polycrystalline samples. This can serve as a useful tool for detecting phase transitions. In order to resolve the structural aspects of the phase transitions detected, hot stage electron microscopy (EM) and electron diffraction (ED) were carried out on a thin transparent single-crystal area. Since cuprous selenide is a mixed conductor, both ionic and electronic, we also report electronic conductivity data, which display anomalies at the phase transitions.

Due to the superstructure the low-temperature ED patterns appear rather complicated but can be indexed within a monoclinic cell with $a = c = 12.30$ Å, $b = 40.74$ Å, and $\beta = (120 \pm 1)°$. ED patterns for a [0 32 $\bar{3}$] monoclinic zone axis are shown in Fig. 2. The ED patterns at room temperature [Fig. 2(a)] are characterized by very strong basic spots, and additional medium-strong and weak spots. Taking into account the basic spots only, a rather good fcc sublattice can be constructed. By comparison with the high-temperature ED patterns [Fig. 2(d)] and x-ray diffraction data[1] we found that the sublattice, formed by the immobile ion framework, is slightly deformed along the [111] direction leading to the appropriate rhombohedral symmetry of the cage.

The high-temperature ED patterns can be easily indexed within the fcc cell.[5] ED patterns, shown in Fig. 2(d) can be treated as for a [112] cubic zone axis and correspond to the fcc cage plus a disordered cation subsystem, usually called α Cu_2Se.

The $\beta \rightarrow \alpha$ transition has been detected at $T_c = 140$ °C. The evidence for the single first-order phase transition is shown in Fig. 1. The linear thermal expansion coefficient clearly reveals a symmetrical peak which is due to the 1.4% volume contraction[1] at T_c. There is also a sharp, order of magnitude, increase of electronic conductivity (σ_e) at T_c. The behavior of σ_e in the α phase is essentially metallic. Ionic conductivity measurements of exactly stoichiometric samples have not yet been carried out.

Considering the ED patterns, shown in Fig. 2, the changes from Fig. 2(a) to Fig. 2(d) were all observed at 140 °C: the basic spots remained although slightly dilatated; the additional spots—super-reflexes vanished and a diffuse halo appeared.

According to the above evidence, the source of the

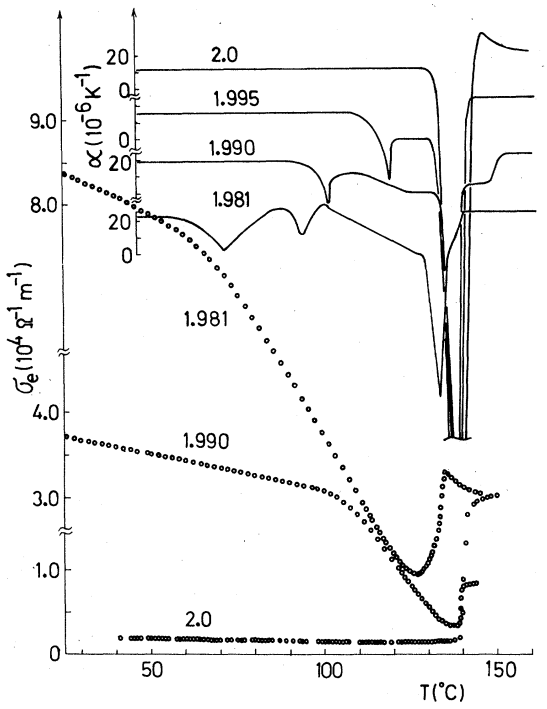

FIG. 1. Linear thermal expansion coefficient (α) vs temperature (full lines) and electronic conductivity (σ_e) vs temperature for various compositions Cu_xSe.

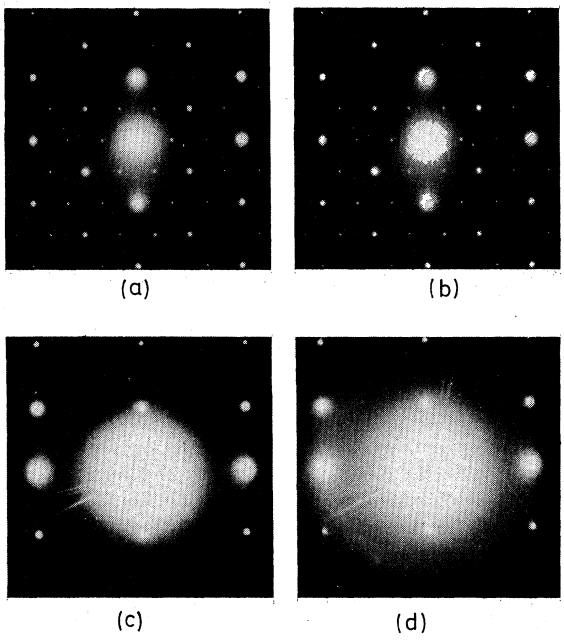

FIG. 2. Sequence of selected area diffraction patterns (SADP's) for $Cu_{1.981}Se$ along [0 32 3] monoclinic zone axis: (a) $\sim 25\,^{\circ}C$; (b) $\sim 80\,^{\circ}C$; (c) $\sim 100\,^{\circ}C$; and (d) $\sim 150\,^{\circ}C$. For $Cu_{1.981}Se$ the full sequence takes place. For $Cu_{1.995}Se$ the pattern (a) changes to (c) at $\sim 120\,^{\circ}C$ and finally to (d) at $\sim 140\,^{\circ}C$. For Cu_2Se the pattern (a) changes to (d) at $\sim 140\,^{\circ}C$. Note: Spot-diameter ratios in (d) fit the fcc values with σ_{rel} two times lower than in (b) and (c). This enables one to treat (d) as SADP for a [112] cubic zone axis.

large latent heat[2] at this transition is still unclear, since only a minor change of the cage was found. Before discussing these results in detail let us discuss the structure of the β phase more carefully.

Beside the rhombohedral periodicity two classes of superperiodicities are extracted from ED and x-ray diffraction analysis: superperiodicity along rhombohedral [111] direction which is the doubled rhombohedral periodicity, and superperiodicity along [220] rhombohedral directions which is tripled rhombohedral periodicity along the same directions. The basic motif which generates the superstructure is a pair consisting of an interstitial Cu ion in octahedral (b) site and nearby vacant tetrahedral (d) site. Formation of such pairs ($d \rightarrow b$; see Fig. 3) stresses one of the $\langle 111 \rangle$ cubic axis causing the rhombohedral deformation of the cage in the same direction. The ($d \rightarrow b$) pairs are hexagonally ordered within the corresponding pair of planes perpendicular to the particular [111] direction in a way to produce the triple superperiodicities. The double superperiodicity along the particular [111] direction (superlattice b axis) can be easily explained by unequal occupation of the neighboring b planes, as shown schematically in Fig. 3. Along the superlattice b axis a pair of ($b \rightarrow d$) planes with an excess ion density is followed by a pair of ($b \rightarrow d$) planes with lower ion density with respect to its mean value in the α phase. Since the ion density (distribution) along superlattice b axis is periodic we may define a modulated ion distribution (MID) along the superlattice b axis. The rhombohedrally deformed fcc cage is most probably a direct consequence of the MID formation.

Concerning nonstoichiometric samples, in the composition range of investigation, the room-temperature ED patterns were all congruent with the stoichiometric one [Fig. 2(a)]. Therefore β-Cu_2Se may be considered as homogeneous within this composition range.

In samples with a slightly lower Cu content two close phase transitions were observed below 140 °C. The evidence for both transitions, thermal expansion, σ_e and ED are shown in Figs. 1 and 2, respectively. The lower-temperature transition is second order, it is detected by ED as a disappearance of super-reflexes and appearance of a diffuse halo [Fig. 2(c)]. These changes indicate the order-disorder character of this transition, in agreement with ionic conductivity mea-

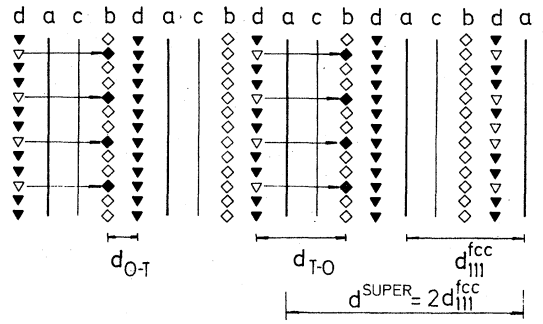

FIG. 3. The planes stacking sequence along the b superlattice axis ($[111]_{fcc}$ direction). Se cage planes—a; Cu cage planes—c; planes of mobile Cu ions: tetrahedrally coordinated—d and octahedrally coordinated—b. The open and full symbols are used to visualize the variation of occupancy between the (a,c,b,d) sandwiches of planes. The arrows indicate pairing between tetraheral vacancies and octahedral ions along the $[111]_{fcc}$ direction.

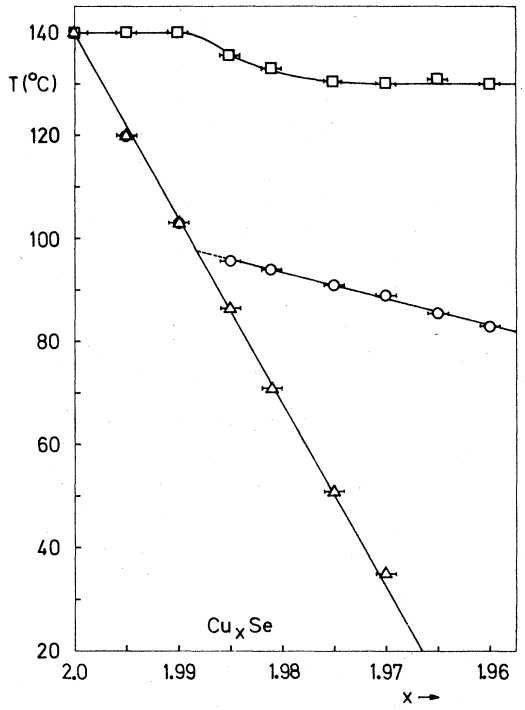

FIG. 4. Equilibrium phase diagram in the vicinity of Cu_2Se; the first-order phase transition (□)—transformation of the immobile ion subsystem; the second-order phase transition (○)—the short-range disordering temperatures and the long-range disordering temperatures (Δ).

surements.[3] The higher transition remains discontinuous, i.e., first order, with two features already found at T_c for stoichiometric samples: the volume contraction and the equalization of cation density along the superlattice b axis, which is essentially an order-disorder transition in b direction. Therefore at this transition we would expect a discontinuous change of σ_i, which is in disagreement with published data.[3] Regardless of the microscopic model we may say that the transition for stoichiometric samples is split under compositional change since all the changes detected for Cu_2Se are preserved but separated between two transitions for $Cu_{2-x}Se$.

Considering the diffraction data we conclude that the second-order phase transition represents essentially an order-disorder transition perpendicular to the b superlattice axis, i.e., within the pair of $b \rightarrow d$ planes (see Fig. 3). This "two-dimensional" disordering does not disturb the ionic organization (MID) along the b superlattice axis which is preserved up to the first-order phase transition but it does break interstitial-vacancy pairs.

Thus we recognize that the prime origin of the first-order phase transition, away from stoichiometry, is the modulated ion distribution along the cubic [111] direction associated with the $b \rightarrow d$ pair of planes (Fig. 3). Therefore at this transition there is a transfer of Cu ions between these pairs of planes. The same reasoning is valid for stoichiometric samples but in this case "two-dimensional" disordering within these planes occurs at the same temperature, thus masking the above type of behavior.

As can be seen in Fig. 4 the temperature of the lower transition, i.e., disordering within the pair of planes falls sharply and linearly with decreasing Cu content. This is understandable since it is expected that a vacancy introduced into a full tetrahedral (d) plane disturbs its surroundings. Therefore the configuration part of the activation energy would be strongly composition dependent lowering the temperature of the onset of "two-dimensional" disordering.

The electronic conductivity σ_e measurements in Fig. 1 show a linear dependence of σ_e above and below the lower transition. At lower temperatures the slope is strongly dependent on composition, but above the transition it is essentially composition independent. This is further evidence that above the lower phase transition the order within a pair of $b \rightarrow d$ planes is destroyed and hence conductivity is no longer sensitive to a small excess of Cu vacancies. A more detailed discussion of the electronic, σ_e, conductivity data, in terms of a hole trapping process, will be given elsewhere.[6]

A further decrease of Cu content beyond $Cu_{1.988}Se$ causes a final splitting of the second-order phase transition into two nondegenerate transitions. As can be seen from Figs. 2(b)–2(d) the splitting concept is still valid since the sum of changes detected at the three transitions can all be found for stoichiometric

samples at the single transition.

The lowest transition on the temperature scale represents the "two-dimensional" disordering only on a long-range scale [Fig. 2(b)]. The accompanying effects which characterize short-range disordering have not been observed at this temperature. Instead, the diffuse halo in ED patterns and the usual low activation energy ($\Delta \simeq 0.12$ eV)[3] for σ_i were observed at the middle line in the phase diagram which therefore represents a short-range disordering.

The observed phase diagram (Fig. 4) is a new contribution to physics of SI conductors since the controlled changes in composition reveal the degenerate nature of $\beta \rightarrow \alpha$ transition of stoichiometric cuprous selenide. Moreover the origin of this transition as well as of the rhombohedral symmetry of the cage seems to be modulated ion distribution (MID) formation. The order parameter (S) comprises two almost independent components ($S_{\parallel}$ and $S_{\perp}$). $S_{\parallel}$ can be easily constructed on the basis of MID and accompanying rhombohedral deformation of the cage. On the other hand, the hexagonal ordering of vacancy-interstital pairs within the $d \rightarrow b$ planes, makes $S_{\perp}$ very sensitive to the composition change since vacancies critically reduce the configurational part of the activation energy for a "two-dimensional" ion mobility.

The above considerations might be valid for other SI conductors which exist only in the stoichiometric form, even if they have a cage symmetry different from the symmetry of the β phase. For these materials other ways must be sought to reveal the degenerate nature of $\beta \rightarrow \alpha$ transition and an essential feature of this transition, the formation of the modulated ion distribution.

ACKNOWLEDGMENTS

We would like to thank Professor S. Barišić, A. Bjeliš, J. Cooper, and J. Przystawa for their stimulating discussions, and I. Aviani and M. Ilić for their assistance. This work received support from the Self-managed Community of Interests in Science, SR Croatia.

[1]O. Milat, Z. Vučić, and Z. Ogorelec (unpublished).
[2]Z. Vučić and Z. Ogorelec, Philos. Mag. B 42, 287 (1980).
[3]T. Takahashi, O. Yamamoto, F. Matsuyama, and J. Noda, J. Solid State Chem. 16, 35 (1976).
[4]M. B. Salamon, in *Physics of Superionic Conductors,* edited by M. B. Salamon (Springer-Verlag, Berlin, 1979), p. 175.
[5]W. Borchert, Z. Kristallogr. Kristallgeom. Krystallphys. Kristallchem. 106, 5 (1945).
[6]Z. Vučić, V. Horvatić and Z. Ogorelec (unpublished).

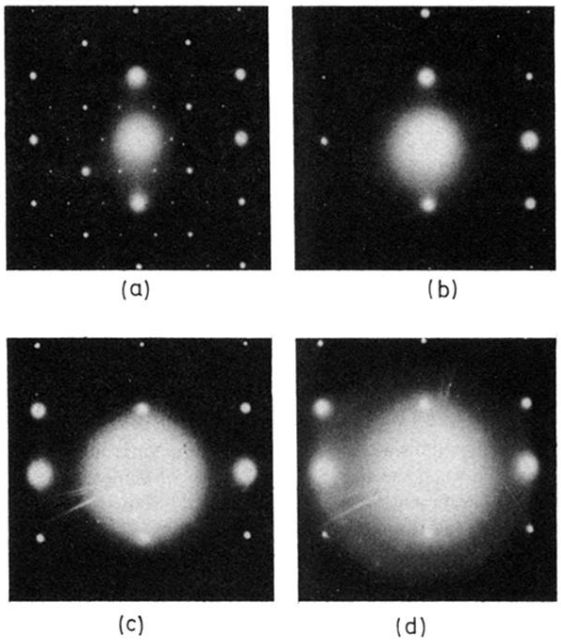

FIG. 2. Sequence of selected area diffraction patterns (SADP's) for $Cu_{1.981}Se$ along [0 32 3] monoclinic zone axis: (a) $\sim 25\,^{\circ}C$; (b) $\sim 80\,^{\circ}C$; (c) $\sim 100\,^{\circ}C$; and (d) $\sim 150\,^{\circ}C$. For $Cu_{1.981}Se$ the full sequence takes place. For $Cu_{1.995}Se$ the pattern (a) changes to (c) at $\sim 120\,^{\circ}C$ and finally to (d) at $\sim 140\,^{\circ}C$. For Cu_2Se the pattern (a) changes to (d) at $\sim 140\,^{\circ}C$. Note: Spot-diameter ratios in (d) fit the fcc values with σ_{rel} two times lower than in (b) and (c). This enables one to treat (d) as SADP for a [112] cubic zone axis.